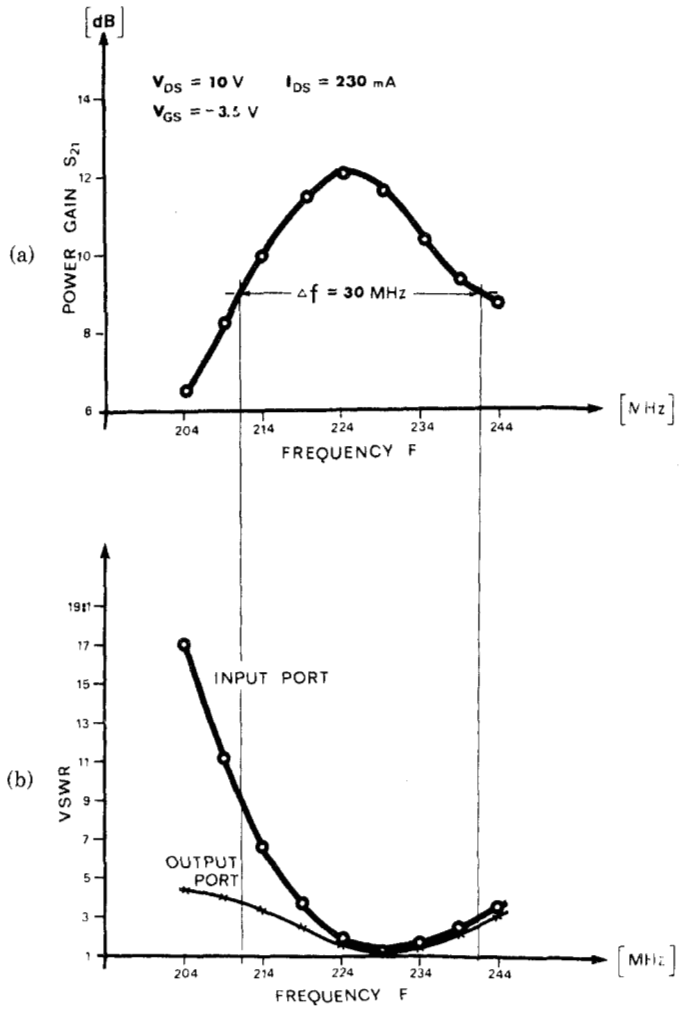

Fig. 4. Small-signal characteristics of RF amplifier. (a) Power gain. (b) Input/output VSWR's.

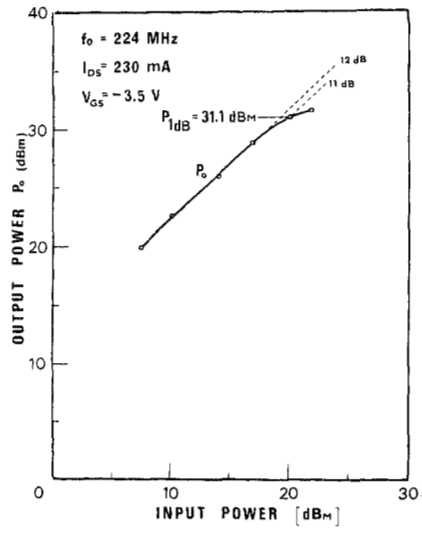

Fig. 5. Large-signal characteristics of RF amplifier.

where P_0 is the total output power in the two signals and P_3 is the power of the intermodulation signal products. With f_0 = 224 MHz and f_1 = 225 MHz and for output power levels below 25 dBm, D_3 is very small and stays 30 dB below the output. However, D_3 starts to increase when the output exceeds 25 dBm. This is probably the result of the drain voltage of the transistor going into the highly nonlinear triode region [2] of the I–V transfer characteristics.

VII. Conclusion

A class-A power amplifier tuned to 224 MHz was constructed using two 30-channel power VFET devices. This amplifier had a linear gain of 12.1 dB up to an output power of 0.8 W and a 1-dB gain compression point of 1.29 W. The distortion characteristics of the amplifier were investigated. The second-harmonic distortion was very low, typically less than 1 percent (−21 dB) even at the 1-dB gain compression point. The third-order intermodulation distortion obtained from a two-tone test was 30 dB below the output in the linear gain region up to an output power level of 0.32 W. Due to a simple structure which results in a high packing density, the power VFET device is capable of handling a large amount of power and is very promising for linear applications since it results in an insignificant amount of second-harmonic distortion and has a low IMD product in the linear power gain region.

References

[1] T. D. Mok and C. A. T. Salama, "A V-groove power JFET for VHF applications," presented at IEDM, Washington, D.C., Dec. 1976.
[2] K. Yamaguchi and H. Kodera, "Optimum design of triode-like JFET's by two-dimensional computer simulation," *IEEE Trans. Electron Devices*, vol. ED-24, pp. 1061–1076, Aug. 1977.

Experimental Determination of Series Resistance of p-n Junction Diodes and Solar Cells

P. J. CHEN, S. C. PAO, A. NEUGROSCHEL, AND F. A. LINDHOLM

***Abstract*—Various methods for determining the series resistance of p-n junction diodes and solar cells are described and compared. New methods involving the measurement of the ac admittance are shown to have certain advantages over methods proposed earlier.**

I. Introduction

The series resistance R_s is a parasitic element in diodes and solar cells that can degrade the device performance. In general, the presence of R_s will bend the current–voltage characteristic away from the idealized characteristic [1]. In a solar cell, this bending decreases the power conversion efficiency [2].

The series resistance of a diode or a solar cell consists of the contact resistances of the metal contacts at both faces of the device and of the resistance of the bulk semiconductor. The resistance of the bulk substrate can be calculated taking into account a spreading resistance correction [3]. The contact resistance is difficult to calculate accurately. In solar cells with a very thin diffused layer and contact grid on the top, the resistance of the diffused layer might dominate. Calculation of this resistance is

Manuscript received June 27, 1977; revised September 10, 1977. This work was supported in part by the NASA-Lewis Research Center under NASA Grant NSG-3019 and in part by the Energy Research and Development Administration under ERDA Contract E(40-1)-5134.

The authors are with the Department of Electrical Engineering, University of Florida, Gainesville, FL 32611.

0018-9383/78/0300-0386$00.75 © 1978 IEEE

difficult because of the nonuniform current flow occurring in the diffused layer [4].

Thus because of the uncertainties and difficulties involved in calculating R_s, methods for direct measurement of R_s are desirable. For a solar cell, a method has been described [5] that involves exposing the solar cell to different illumination levels. Here we describe three other methods for measurement of R_s which can be applied to any diode or solar cell. These methods involve:

a) small signal admittance measurement at moderately high frequency
b) combined measurement of dc and ac conductance
c) open-circuit-voltage-decay measurement (OCVD).

II. Theory

The small-signal equivalent model of the ideal junction diode, derived by Shockley [1], consists of a diode conductance G_{QN} and a diode capacitance C_{QN} in parallel. The circuit elements, G_{QN} and C_{QN}, result from solving the continuity equation for holes and electrons under small-signal excitations including both the *quasineutral* base and emitter regions. In parallel with these two elements, the circuit representation of a real diode includes two capacitances originating in the junction space-charge region: C_T, associated with the ionized impurities, and C_{SCR}, associated with the mobile charges [6]. The total capacitance is $C_D = C_{QN} + C_T + C_{SCR}$. To complete the circuit, R_s is added, as shown in Fig. 1(a).

Method a): G_D increases exponentially with increasing bias voltage V_D [1], whereas as shown by Sah [6], for small forward bias, $C_D \simeq C_T$ shows a relatively weak dependence of V_D. If the small-signal admittance of the diode is measured at a forward bias small enough and at a frequency ω high enough so that $\omega C_D \gg G_D$, then the diode equivalent circuit reduces to R_s and C_D in series, as shown in Fig. 1(b). R_s can be easily measured using a suitable high-frequency (1 to 10 MHz) bridge.

Method b): In contrast to method a), we now set the forward-bias voltage V and the frequency ω to such values that $\omega C_D \sim G_D$. Noting that an admittance bridge measures G_P and C_P of the parallel combination shown in Fig. 1(c), we see that the dependence of G_P plotted against V will differ from the dependence of G_D against V because of the presence of R_s. For dc conditions, as illustrated in Fig. 1(d), the measured conductance $G_{DC} = [R_s + 1/G_D]^{-1}$ will show yet another dependence on V. Comparison of $G_P(V,R_s)$ versus $G_{DC}(V,R_s)$ then yields R_s. A simple computer program can be written to enable rapid determination of R_s.

Method c): The open-circuit-voltage-decay (OCVD) measurement [7] has been often used to determine minority carrier lifetime of a diode. In this measurement, a voltage step applied in the forward direction causes a flow of forward current I. The terminals are then open-circuited. The resulting cessation of I causes a sharp drop of the voltage ΔV to occur at the diode terminals. This voltage drop ΔV divided by I gives series resistance R_s [7].

III. Results

Table I shows results from methods a) and c) together with data obtained by the illumination method of Wolf and Rauschenbach [5]. The devices used in the measurements were p^+-n silicon diodes, 30 mil in diameter and 2×2 cm^2 n^+-p solar cell. The OCVD method was inaccurate for the devices measured since the voltage drop ΔV was difficult to determine accurately; this is especially difficult in devices with short lifetimes. Method b) could not be used for our devices, since the ac measurements have to be taken at a frequency ω such that $\omega \ll 2/\tau$ [1], where τ is the minority carrier lifetime in the base. In the devices we studied, τ was a few microseconds which requires measurement at frequencies not exceeding about 5 kHz. At such low frequencies, G_P will differ from G_{DC} by only about 0.005 percent, which is much less than the estimated experimental accuracy of 1 percent.

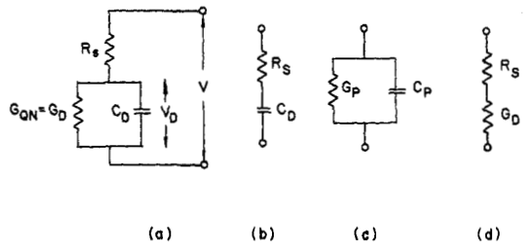

Fig. 1. (a) AC equivalent circuit. (b) High-frequency equivalent circuit for $\omega C_D \gg G_D$. (c) Parallel equivalent circuit as measured by bridge, where G_P, C_P are functions of G_D, C_D, R_s, ω. (d) DC equivalent circuit.

TABLE I
Series Resistance from Methods a) and c) Together with Results Using Light Excitation for Comparison

	Series resistance R_s in ohms		
Device	Method (a)	Method (c)	Photovoltaic output [5]
p^+-n diode			
10Ωcm, 30 mil. dia.	20	19-28	15-23
p^+-n diode, 30 mil. dia.			
0.1Ωcm	4.35	3-10	3.5-4.5
2x2 cm^2 n^+-p solar cell			
2Ωcm	0.33	~0.6	0.25-0.34

This method can be used, however, for short-lifetime devices. For example, if $\tau = 0.1$ μs, the ac measurements could be done at a frequency of a few hundred kilohertz, at which $G_P - G_{DC}$ would be large enough to enable a determination of R_s.

Method a) is the simplest approach and gives accurate results that agree reasonably well with those produced by the illumination method. The accuracy of method a) is limited by the accuracy of the bridges used, which is better than five percent for the meaurements reported here. Measurements were taken at frequencies between 1 and 5 MHz. The results obtained from the illumination method depend on the light intensity [5]; the values of R_s determined by this method fall in the range indicated in Table I. In contrast to the illumination method, method a) involves only electrical excitation and applies to ordinary diodes as well as to solar cells.

The high-frequency measurements were done on Wayne-Kerr B601 and B801 bridges; low-frequency measurements were done on a Wayne-Kerr B224 bridge.

IV. Summary

This work demonstrates a simple and rapid method (method a)) for determining the series resistance of diodes and solar cells based on the measurement of small-signal admittance. The OCVD method (method c)) provides a rapid but coarse estimate of R_s. Method b) is useful for devices having a short substrate lifetime. Method b) enables also measurement of R_s at any bias voltage V, which allows the determination of any dependence that R_s might have on V.

References

[1] W. Shockley, "The theory of p-n junctions in semiconductors and p-n junction transistors," *Bell Syst. Tech. J.*, vol. 28, pp. 435–489, July 1949.

[2] M. B. Prince, "Silicon solar energy converters," *J. Appl. Phys.*, vol. 26, pp. 534–540, May 1955.
[3] G. F. Foxhall and J. A. Lewis, "The resistance of an infinite slab with a dioelectrode," *Bell Syst. Tech. J.*, pp. 1609–1619, July 1964.
[4] R. J. Handy, "Theoretical analysis of the series resistance of a solar cell," *Solid-State Electron.*, vol. 10, pp. 765–775, 1967.
[5] M. Wolf and H. Rauschenbach, "Series resistance effects on solar cell measurements," *Advanced Energy Conversion*, vol. 3, pp. 455–479, Apr.–June 1963.
[6] C. T. Sah, "Effects of electrons and holes on the transition layer characteristics of linearly graded p-n junction," *Proc. IRE*, vol. 49, pp. 603–618, Mar. 1961.
[7] S. R. Lederhandler and L. J. Giacoletto, "Measurement of minority carrier lifetime and surface effects in junction devices," *Proc. IRE*, vol. 43, pp. 477–483, Apr. 1955.

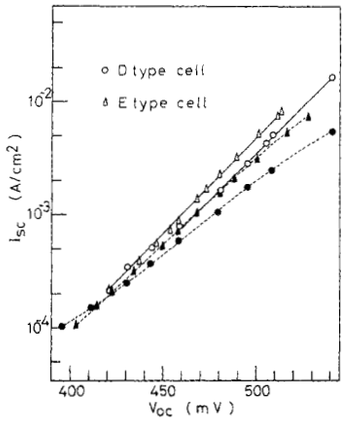

Fig. 1. Short-circuit current versus open-circuit voltage (full lines) at various illumination intensities and current–voltage characteristics (dotted lines) at dark condition. O: D type cell. Δ: E type cell.

Epitaxial Silicon Solar Cells with Uniformly Doped Layer

AKIRA USAMI AND SHINICHIRO ISHIHARA

***Abstract*—Solar cell structures have been prepared both by successive deposition of p-type and n-type silicon layers on p^+-type single-crystal silicon. Impurities are uniformly doped at epitaxial layers. Efficiency of 9.0 percent with the epitaxial layer junction structure and 12.8 percent with the diffused 0.3-μm junction depth structure have been achieved.**

Various silicon epitaxial solar cells have been reported in the literature [1]–[5]. D'Aiello *et al.* [1] have reported the p^+-p-n-n^+ structure epitaxial solar cells which have graded n-base region. AR coating is Al_2O_3 of 700 Å in thickness. Open-circuit voltage, fill factor, and AM1 efficiency are 636 mV, 0.79, and 12.6 percent, respectively. The effective saturation current density of the epitaxial junction has been very low ($I_0 = 9 \times 10^{-13}$ A/cm^2) and the open-circuit voltage of 636 mV has been the highest value that has been reported. Epitaxial silicon solar cells on metallurgical silicon have been reported by Chu *et al.* [2]. Metallurgical-grade silicon with a purity of 98–99 percent costs about \$1/kg. Although the epitaxial layer is structurally much superior to the substrate material [4], the efficiency of the solar cell has been 3.4 percent at AM0 (V_{oc} = 540 mV, I_{sc} = 15 mA/cm^2, and F.F. = 0.67). Cells of Chu *et al.* [4] are very cheap but too low in efficiency to be used for commercial power supply, and D'Aiello *et al.*'s [1] have impurity gradient in epitaxial layer, so they cannot be mass-produced and may be expensive. Kressel *et al.* [5] have prepared epitaxial solar cells on cheap EFG "ribbon" substrate, the cell has the drift field in the epitaxial layer. This correspondence reports on relatively cheap epitaxial silicon solar cells with uniformly doped epitaxial layer.

n^+-type and p^+-type substrates were made of (111) oriented single-crystal silicon with a resistivity of <0.02 Ω·cm and a thickness of 200–300 μm. The diffused junction structure (D type) cell was boron diffused into the n-type epitaxial region, the thickness of which was 34.2 μm and the resistivity 11.3 Ω·cm, which was grown on n^+-substrate. Boron diffusion was done at 1150°C for 60 min, 10 cm^3/min. Dry nitrogen was flowed through BBr_3 and then mixed with the main gas, which consisted of 100 cm^3/min of oxygen plus 1000 cm^3/min of nitrogen. The epitaxial layer junction structure (E type) cell was made by growing a n-type epitaxial layer (thickness of about 1 μm and resistivity <0.1 Ω·cm), on a p-type epitaxial layer. The thickness of the p-type epitaxial layer is 30 μm and the resistivity is about 10 Ω·cm on the p^+-type substrate. Epitaxial layer was grown by using trichlorosilane as the silicon source in a standard horizontal reactor. Dopants for the p-type and n-type epitaxial layers was boron and phosphorus, respectively. Grid-shaped ohmic contacts were evaporated on the front surface of the cells. The cell fabrication was completed by mesa etching. AR coating was not applied. Details of samples are shown in Table I.

Manuscript received July 6, 1977; revised November 7, 1977.
The authors are with the Department of Electronics, Nagoya Institute of Technology, Gokiso-cho, Showa-ku, Nagoya, Japan.

TABLE I
Device Fabrication Conditions and the Device Characteristics of the D and E Type Solar Cells

	D type cell	E type cell
Surface layer	1150°C 60min. Boron diff.	n^+-type <0.1Ω-cm ~ 1μm
Base layer	n-type 11.3Ω-cm 34.2μm	p-type 10Ω-cm 32.5μm
Substrate	n^+-type <0.02Ω-cm 300μm	p^+-type <0.015Ω-cm 200μm
Dark condition	n=1.39 I_o=1.0x10^{-9}A/cm^2	n=1.10 I_o=2.3x10^{-10}A/cm^2
Illuminated condition	n'=1.0 I_o'=2x10^{-11}A/cm^2	n'=1.0 I_o'=4x10^{-11}A/cm^2
Sunlight density	54.5mW/cm^2	78.9mW/cm^2
Opencircuit voltage	530mV	501mV
Shortcircuit current	18.6mA/cm^2	19.2mA/cm^2
Fill factor	0.710	0.740
Efficiency (active area)	12.8% (1.7cm^2)	9.0% (0.85cm^2)
AR coating	No	No

Solid lines in Fig. 1 show the current–voltage characteristics of the D and E type cells obtained by variation of the illumination intensity with a change of distance between a cell and a tungsten-filament lamp and measurement of the short-circuit current density as a function of the open-circuit voltage. Dotted lines are the dark-condition current–voltage characteristics. The n' value (distinguished from the dark-condition n value) was 1.0 and the effective saturation current density, I_0', which is defined by the following equation, was $2 - 4 \times 10^{-11}$ A/cm^2.

$$I_L = I_0' \exp(qV_{oc}/n'kT).$$

Typical values obtained for n,n',I_0, and I_0' are also tabulated in